Electronic Supplementary Material (ESI) for Catalysis Science & Technology.

Supplementary Information

Low quantum efficiency of μ-oxo iron bisporphyrin photocatalysts explained with femtosecond M-edge XANES

Kori M. Sye,† *Clare A. Leahy,*† *& Josh Vura-Weis**

Department of Chemistry, University of Illinois at Urbana-Champaign

600 S. Matthews Ave., Urbana, IL 61801

Contents

Supplementary Information 1
General Materials and Methods 2
Optical Transient Absorption 2
Experimental Details 2
Wavelength dependent dynamics 3
Solvent-Dependent Dynamics 6
Ground State & Transient M-edge XANES 8
CTM4XAS Simulations 8
References 11

General Materials and Methods

5,10,15,20-tetraphenyl-21H,23H-porphine iron(III) chloride (FeTPPCl) was purchased from Sigma Aldrich. The stacked porphyrin μ-oxo-bis[(tetraphenylporphinato)iron(III)] ($(TPPFe)_2O$) was made following literature procedures.[1–3] All other chemicals were purchased and dried according to literature procedures before use. Concentrated thin films of $(TPPFe)_2O$ and FeTPPCl embedded in polystyrene were made following a modified literature procedure[4] as follows: A concentrated solution of the target compound dissolved in dichloromethane was filtered to remove undissolved particulates; this solution was then mixed with a filtered 4% polystyrene solution in DCM in ~5:1 ratio. 50-100 uL (~2 drops) of this mixed solution was placed onto a cleaned glass coverslip, which was then slipcoated using a second cleaned glass coverslip and air dried to form ~300-400nm thick polymer films (absorbance of ~0.4-1.0 at the desired excitation wavelength). These were then floated off the glass using water and placed on sample frames for use. Static UV-Vis spectra were taken to confirm sample identity and determine the thickness and relative concentration of the compound embedded in the polystyrene film. Additional samples of ~100 nm FeTPPCl thin films were deposited on 50 nm Si_3N_4 membranes via thermal evaporation using a house-built instrument. Static UV/Vis spectra were taken to confirm the sample identity. Global analysis for all transient experiments was performed using Glotaran[5] to extract the component spectra of the excited states.

Optical Transient Absorption
Experimental Details

Optical transient absorption spectroscopy of $(TPPFe)_2O$ in degassed, anhydrous benzene was performed pumping at 400 nm, 350 nm, and 325 nm. The optical transient absorption spectroscopy was performed with broadband, approximately 100 fs, probe pulses generated through white light generation from 35-fs, 800 nm pulses (Spectra-Physics Ace) focused into a sapphire plate. The white light is transmitted through the sample and refocused onto a spectrometer. The 400 nm pulses are generated via SHG in a BBO crystal from the 800 nm fundamental, while 350 and 325 nm pulses were generated by doubling the 700 and 650 nm output of a nonlinear optical parametric amplifier (TOPAS White). All samples were pumped to an excitation fraction of 2-10% per

porphyrin monomer, with ~1 μJ of the pump pulse focused to ~320 μm. The time resolution is approximately 100 fs.

Wavelength dependent dynamics

Optical transient absorption spectroscopy was performed at three excitation wavelengths (400 nm, 350 nm, and 325 nm) to verify that substantially similar photophysics are observed at each energy. Figure S1a shows a contour plot of the optical transient absorption spectra of the bisporphyrin in benzene, pumped at 400 nm. Figure S1b reproduces Figure 2A from the main paper for easier comparison of the spectra with those of other pump wavelengths below.

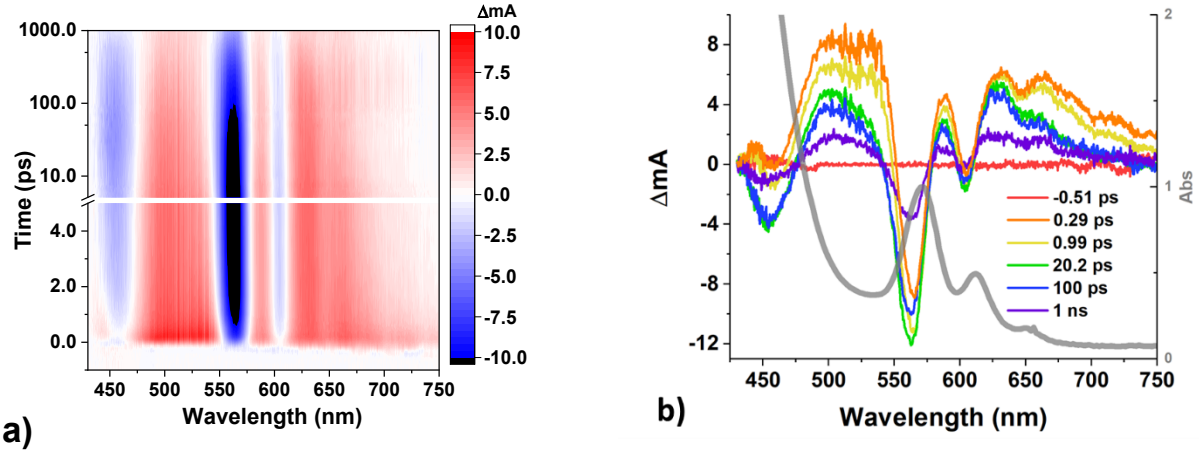

Figure S1 – (a) Contour plots of the transient optical absorption of the bisporphyrin in benzene pumped at 400 nm. (b) Slices at select time delays (reproduced from Figure 2A in the main paper)

Figure S2 shows transient absorption spectra of the bisporphyrin embedded in polystyrene film after 400 nm excitation as (a) a contour plot and (b) selected time slices. Comparison of the polystyrene and benzene solution are given in Figure S9 in the "Solvent-Dependent Dynamics" section.

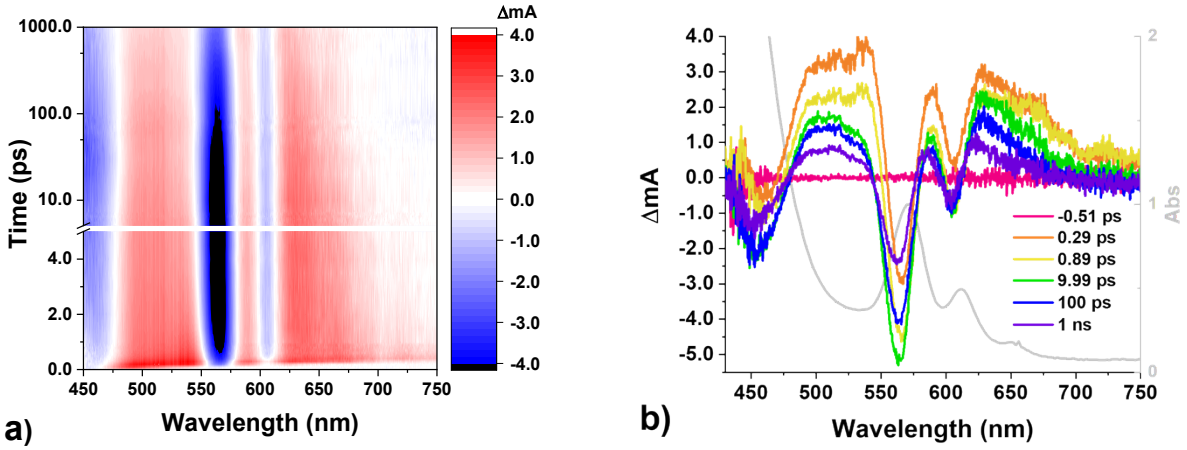

Figure S2 – (a) Contour plots of the transient optical absorption of the bisporphyrin embedded in polystyrene (PS) pumped at 400 nm. (b) Spectral slices at select time points. The static UV-Vis spectrum of the stacked porphyrin $(TPPFe)_2O$ is plotted in grey.

Figure S3 shows transient absorption spectra after 350 nm excitation as (a) a contour plot and (b) selected time slices. Figure S4 shows the component spectra after a global fit using a 3-state sequential model. These are nearly identical to the component spectra after 400 nm excitation shown in Figure 2B of the main paper.

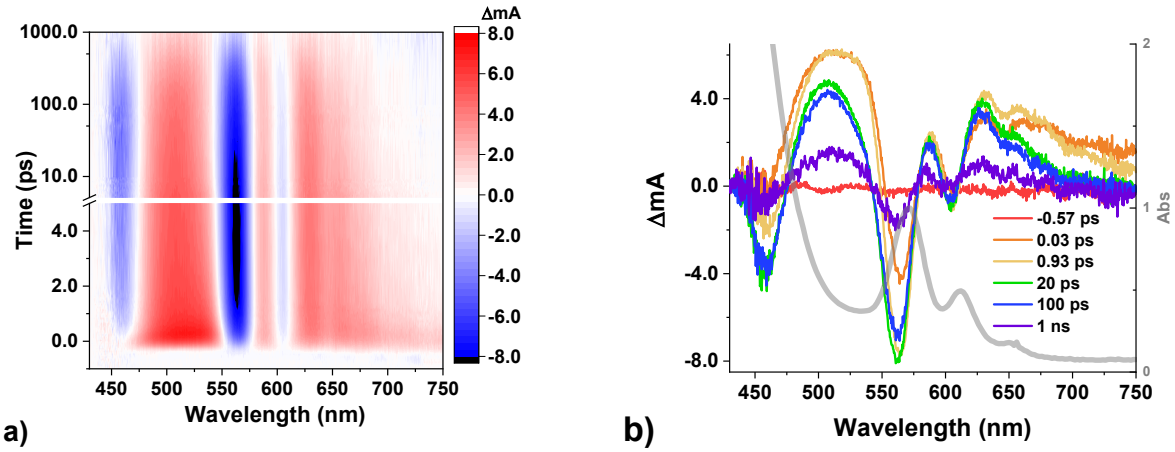

Figure S3 - (a) Contour plots of the transient optical absorption of the bisporphyrin in benzene pumped at 350 nm. (b) Spectral slices at select time points. The static UV-Vis spectrum of the stacked porphyrin $(TPPFe)_2O$ is plotted in grey.

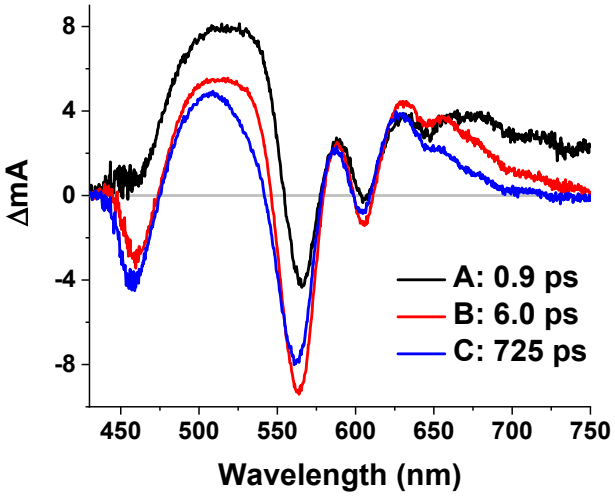

Figure S4 - Component species associated decay spectra (SADS) obtained from the global analysis of a 3-state sequential model of the bisporphyrin transient visible absorption in benzene pumped at 350 nm.

Figure S5 shows transient absorption spectra after 325 nm excitation as (a) a contour plot and (b) selected time slices. Figure S6 shows the component spectra after a global fit using a 3-state sequential model. The first component shows a higher excited-state absorption signal at 475 nm than after 400 nm or 350 nm excitation, possibly indicating more LMCT character in the initial excited state. The latter two component spectra are nearly identical to those shown in Figures S3 and Figure 2B from the main paper, indicating that the later states are likely the same as in the longer-wavelength pumps.

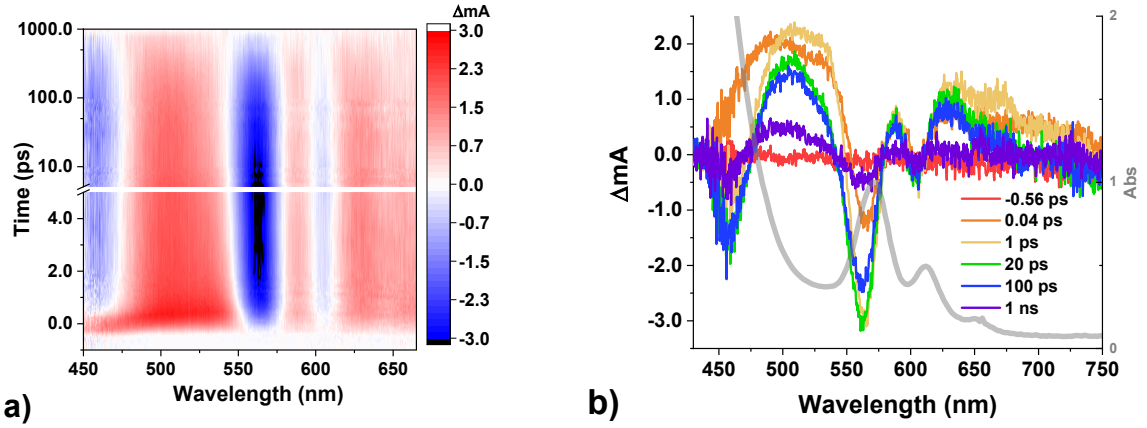

Figure S5 - (a) Contour plots of the transient optical absorption of the bisporphyrin in benzene pumped at 325 nm. (b) Spectral slices at select time points. The static UV-Vis spectrum of the stacked porphyrin $(TPPFe)_2O$ is plotted in grey.

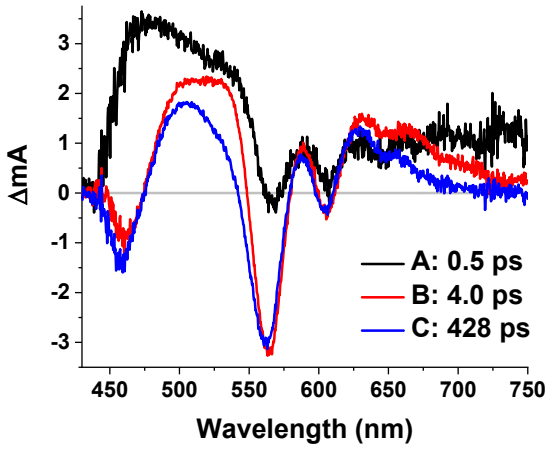

Figure S6 – Component species associated decay spectra (SADS) obtained from the global analysis of a 3-state sequential model of the bisporphyrin transient visible absorption in benzene pumped at 325 nm.

Table S1 summarizes the lifetimes obtained from the global fits – all show a ~1 ps fast decay from state A to B, then a few-ps and few-hundred ps lifetimes of the next two states. The latter two lifetimes appear to accelerate as the pump energy increases, which may be due to additional vibrational energy in states B and C from the higher-energy pump. We will investigate this wavelength dependence in greater detail in future work. For the present work, we conclude based on the nearly identical State B and C component spectra at all pump energies that the general excited-state dynamics are similar at all pump energies.

Excitation λ (nm)	**τ_X (ps)**	**τ_Y (ps)**	**τ_Z (ps)**
400	0.97 ± 0.02	8.2 ± 0.3	846 ± 8
350	0.91 ± 0.02	6.0 ± 0.2	725 ± 5
325	0.51 ± 0.02	4.0 ± 0.1	428 ± 7

Table S1 - Lifetimes of $(TPPFe)_2O$ optical excited states X, Y, Z from global kinetic analysis at different pump wavelengths (benzene)

Figure S7 is the reconstructed simulated data from the global analysis of the transient optical absorption of the bisporphyrin in benzene using 400 nm pump excitation as an example in comparison to the experimental data, demonstrating that the global analysis model matches the experimental data.

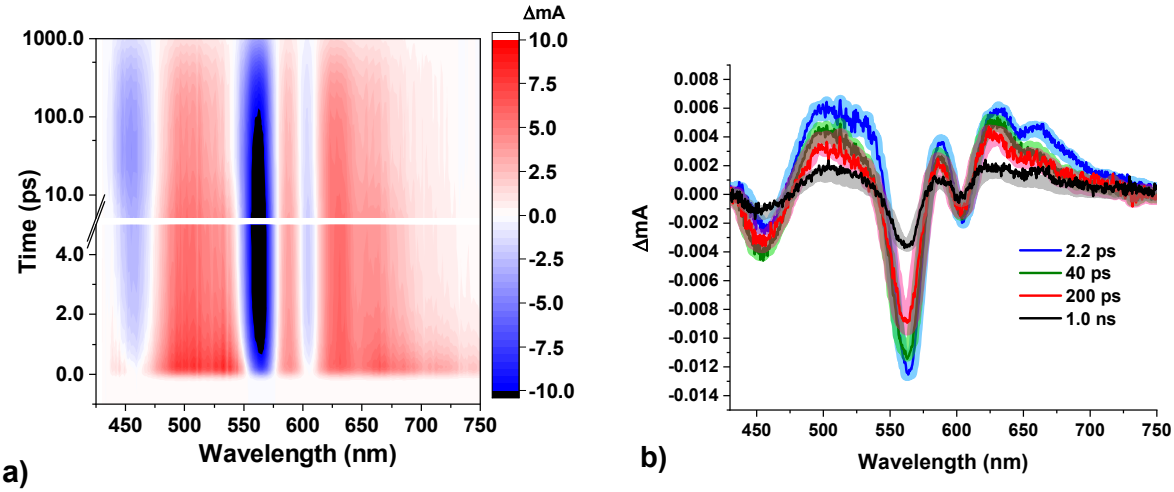

Figure S7 – (a) Recreated contour plot from global analysis of the transient optical absorption of the bisporphyrin in benzene pumped at 400 nm. (b) Comparison of experimental data (solid lines) to the species associated decay spectra (SADS, transparent lines) derived from the global analysis of OTA of the bisporphyrin in benzene with 400 nm excitation, finding excellent agreement between the experimental data and the global analysis model.

Solvent-Dependent Dynamics

To determine if the photodynamics of $(TPPFe)_2O$ were solvent-dependent, and therefore whether it is reasonable to equate the transient M-edge XANES performed on embedded polymer films with solution-phase photochemistry, optical transient absorption dynamics were performed using solutions of the bisporphyrin in benzene, dichloromethane (DCM), and tetrahydrofuran (THF). Additional excitation wavelengths (350 & 325 nm) were also investigated, as prior work has shown a minor wavelength dependence on photon-to-product efficiency; increased pump energy led to increased efficiency, if still poor.[6] These samples were prepared using the appropriate degassed, anhydrous solvents and checked by UV-Vis before and after excitation by 400 nm, 350 nm, or 325 nm pump to ensure no sample damage had occurred. We also performed OTA of the bisporphyrin embedded in a polystyrene matrix to match the conditions of the transient XUV experiment. Due to the current limitation of the XUV instrument to thin film samples, this was crucial for determining if the same dynamics occur in solution and in the embedded film for comparison of OTA and transient M-edge XANES.

As shown in Figure S8, the dynamics are generally similar across all pump energies and solvent environments. Tables S2-S4 summarize three-exponential fits for each experiment at probe wavelength 515 nm – while there are small changes in the time constants between the experiments, the overall picture consistent in all cases is of an initial sub-picosecond decay, followed by ten-to-hundreds of ps and ~1 ns decays. Note in all cases that the third exponential is approximate since data was only collected to 1

ns. Figure S9 additionally shows comparison of single wavelength kinetic analysis at 515, 565, and 590 nm for polystyrene and benzene in closer detail, showing similar kinetic fits and indicate dynamics are similar between the two matrices. The lifetimes derived from the respective kinetic analyses at those wavelengths for the polystyrene and benzene matrices are summarized in Table S5. The minor changes in dynamics between solvent environment suggest that changes to the local environment about the bisporphyrin influence the dynamics to some degree, suggestive that larger changes in terms of ligand structure may have a large impact on the branching ratio between the Fe(III) ion pair and the Fe(II)/Fe(IV)-oxo states. Fit errors are the reported errors from Levenberg–Marquardt fits, which in our experience underestimate the true error of the experiment. The pump fluence and excitation % is also shown for each experiment; because of slight solvatochromism of the Soret band the excitation fraction differs between solvents even with the same pump fluence.

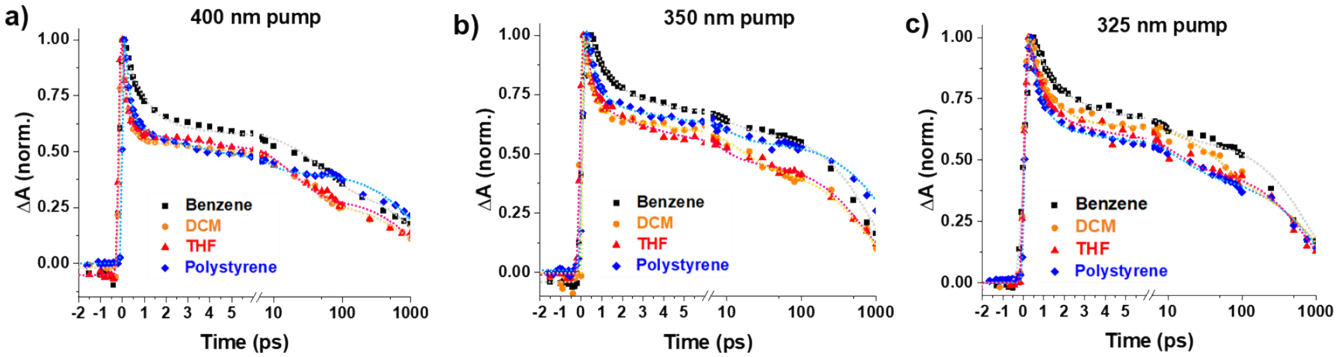

Figure S8 - Normalized time traces at 515 nm after excitation at (a) 400 nm, (b) 350 nm, and (c) 325 nm in various solvents with the respective kinetic fits given as dotted lines.

Solvent	τ_1 (ps)	τ_2 (ps)	τ_3 (ps)	Pump fluence (mJ/cm^2)	Excitation %
Benzene	0.79 ± 0.07	44 ± 8	1558 ± 246	1.4	11
DCM	0.25 ± 0.01	27 ± 2	1110 ± 60	0.7	7
THF	0.19 ± 0.02	19 ± 2	1240 ± 70	0.7	5
Polystyrene	0.23 ± 0.02	4.9 ± 0.5	1330 ± 74	0.8	3

Table S2 - Kinetic analysis at 515 nm after 400 nm excitation.

Solvent	τ_1 (ps)	τ_2 (ps)	τ_3 (ps)	Pump fluence	Excitation %

				(mJ/cm²)	
Benzene	0.9 ± 0.2	7 ± 2	940 ± 30	1.7	4
DCM	0.2 ± 0.1	11 ± 4	880 ± 140	1.7	4
THF	0.36 ± 0.04	5.5 ± 0.5	750 ± 35	1.7	4
Polystyrene	0.45 ± 0.06	7.6 ± 1.6	1676 ± 56	1.5	4

Table S3 - Kinetic analysis at 515 nm after 350 nm excitation.

Solvent	τ_1 (ps)	τ_2 (ps)	τ_3 (ps)	Pump fluence (mJ/cm²)	Excitation %
Benzene	0.9 ± 0.3	7 ± 3	830 ± 40	0.9	3
DCM	0.89 ± 0.07	54 ± 10	1100 ± 70	0.9	2
THF	0.7 ± 0.1	11 ± 3	820 ± 44	0.9	2
Polystyrene	0.56 ± 0.05	14.4 ± 2.6	956 ± 41	1.2	2

Table S4 - Kinetic analysis at 515 nm after 325 nm excitation.

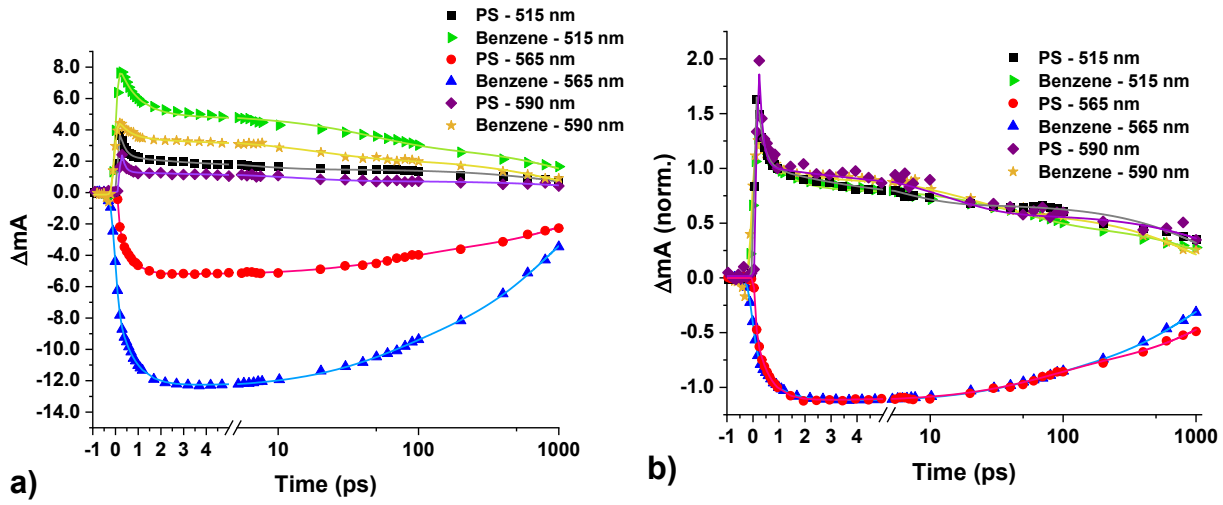

Figure S9 – Comparison of kinetics of the transient optical absorption of the bisporphyrin in polystyrene versus benzene at 515, 565, and 590 nm probe wavelengths at 400 nm excitation, showing the unnormalized (a) and normalized (b) overlays. Experimental data are given as scatter points, while the respective kinetic fits are given as solid lines in the same color.

Probe λ (nm)	Matrix	τ_1 (ps)	τ_2 (ps)	τ_3 (ps)
515	*Benzene*	0.79 ± 0.07	44 ± 8	1560 ± 250
	Polystyrene	0.23 ± 0.02	4.9 ± 0.5	1330 ± 74
565	*Benzene*	0.75 ± 0.02	56 ± 5	930 ± 20
	Polystyrene	0.52 ± 0.02	70 ± 7	1770 ± 110
590	*Benzene*	0.5 ± 0.3	19 ± 5	1100 ± 120
	Polystyrene	0.14 ± 0.02	13 ± 3	2000 ± 400

Table S5 - Kinetic analysis of the bisporphyrin in benzene versus polystyrene at 515, 565, and 590 nm after 400 nm excitation.

Ground State & Transient M-edge XANES

The tabletop XUV probe was generated through the process of high-harmonic generation (HHG) as described in prior works.[4,7,8] The 1 kHz, 35 fs, 800 nm pulse of the NIR driving laser is focused into a semi-infinite gas containing approximately 100 Torr of Neon to generate approximately 20 fs XUV pulses in the energy range from 40-90 eV.[7] The residual NIR pulses were filtered using a 100 nm thick Al foil and creating a flux of 10^5 photons per pulse are available at the sample position. [8] The spectrometer resolution is measured using the absorption lines of Xe and Xe^+ and has been found to be near 0.4 eV FWHM for these experiments. Transient absorption of a thin film of Fe_2O_3 is used to determine the instrument response function (IRF) of 90 fs FWHM. The pump fluence of 1.6 mJ/cm^2 at 400 nm corresponds to an average excitation fraction of ~8% per individual porphyrin. Pump fluences from 0.8 to 2.7 mJ/cm^2 were tested, but no significant variation in the transient dynamics of the stacked porphyrin were observed.

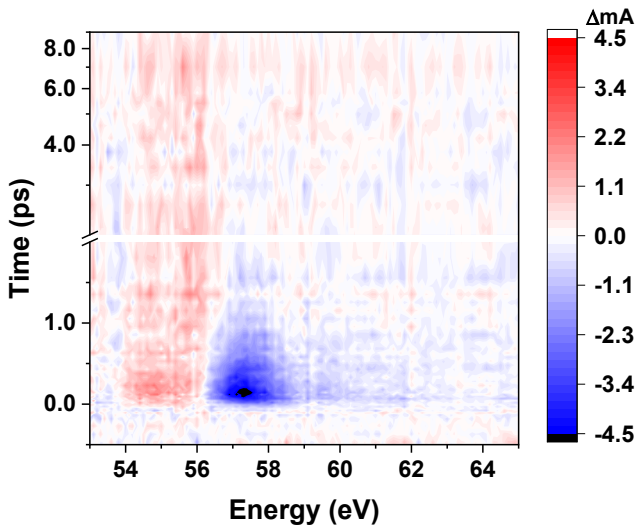

Figure S10 - Transient $M_{2,3}$-edge XANES contour plot of $(TPPFe)_2O$ pumped at 400 nm.

CTM4XAS Simulations

To assist in the identification of the observed excited state dynamics, the $M_{2,3}$-edge transitions were simulated for the proposed $(TPPFe)_2O$ excited states using a locally modified version of the program CTM4XAS that calculates the linewidth of each final state.[9-10] While the overall complex is antiferromagnetic, each iron is considered separately as a high spin iron(III) in a square planar (D_{4h}) ligand field. The broadband XUV probe excites a set of symmetry-allowed 3p→3d transitions. Electron-electron repulsion splits the $3p^6$-$3d^5$ ground state and $3p^5$-$3d^6$ core-hole state into the Russel-Saunders states shown. These states are further split due to the symmetry of the ligand field, accounted first through the octahedral field splitting followed by the square planar field splitting as a perturbation on the octahedral field – parameters were derived from Ryland *et al* 2018.[8] While other ligand field parameters were tested, these were found to be the best fit for the experimental HS Fe(III) spectrum. These parameters were also used to calculate versions with an iron(II) centre and iron (IV) centre. To account for a strong-field oxo ligand, stronger ligand field parameters were used to calculate an intermediate-spin (S = 1) Fe(IV) centre for the Fe(IV)=O. The resulting ligand field states are designated by the appropriate Mulliken term symbols. Spin-orbit coupling (SOC) further splits the ligand-field strength. The allowed transitions are determined using the point group-

specific transition moment integral. The simulation also includes transition-specific Lorentzian lifetime broadening and 0.2 eV FWHM Gaussian broadening to account for the spectrometer resolution. The LFM method does not calculate absolute peak energies accurately, so the Fe(III) centre simulation is shifted to match the experimental peak and the others adjusted by the same shift. Finally, a Fano lineshape with q=3.5 is applied to account for interference between direct photoemission and Auger pathways. Primary simulation parameters are shown in Supplementary Table S5, while additional details on the calculation are given in a previous publication.

	Term Symbol	**Charge**	**Scaling of Slater integrals**			**SOC**	**Crystal Field Parameters**		
			fdd	*fpd*	*gpd*		*10Dq*	*Ds*	*Dt*
S = 5/2	$^6A_{1g}$	3+	1	0.625	0.625	1	2.5	.15	.07
S = 2	$^5A_{1g}$	2+	1	0.625	0.625	1	2.5	.15	.07
S = 2	$^5A_{1g}$	4+	1	0.625	0.625	1	2.5	.15	.07
S = 1	$^3A_{1g}$	4+	1	0.625	0.625	1	4.8	.05	.70

Table S5 - Parameters for CTM4XAS simulations for the potential iron centres in the excited states of $(TPPFe)_2O$ – derived from a prior publication.[8]

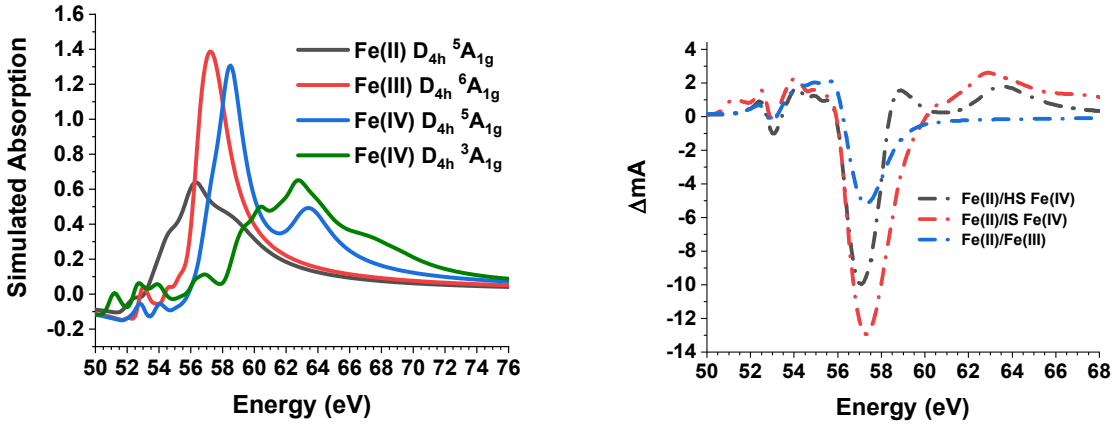

Figure S11 - (a) The CTM-simulated ground state of D_{4h} iron porphyrin with oxidation states 2+ (black), 3+ (red), and 4+ (IS green, HS blue). (b) The simulated excited states

of predicted combinations of iron oxidations states in the potential excited states of $(TPPFe)_2O$. The red plot depicts an excited state containing a Fe(II) and intermediate-spin Fe(IV) centre with an 8% excitation fraction. The blue plot depicts an excited state containing and Fe(II) and an Fe(III) centre with an 8% excitation fraction. The black plot depicts the excited state spectrum containing a Fe(II) and high-spin Fe(IV) state given the 8% excitation fraction.

References

1 E. B. Fleischer and T. S. Srivastava, *J. Am. Chem. Soc.*, 1969, **91**, 2403–2405.

2 A. B. Hoffman, D. M. Collins, V. W. Day, E. B. Fleischer, T. S. Snvastava and J. L. Hoard, *J. Am. Chem. Soc.*, 1972, **94**, 3620–3626.

3 J. H. Helms, L. W. Ter Haar, D. L. Harris, W. E. Hatfield, K. Jayaraj, G. E. Toney, A. Gold, T. D. Mewborn and J. R. Pemberton, *Inorg. Chem.*, 1986, **25**, 2334–2337.

4 Y. Shari'ati and J. Vura-Weis, *J. Synchrotron Radiat.*, 2021, **28**, 1850–1857.

5 J. J. Snellenburg, S. Laptenok, R. Seger, K. M. Mullen and I. H. M. van Stokkum, *J. Stat. Softw.*, 2012, **49**, 1–22.

6 M. W. Peterson, D. S. Rivers and R. M. Richman, *J. Am. Chem. Soc.*, 1985, **107**, 2907–2915.

7 K. Zhang, M. F. Lin, E. S. Ryland, M. A. Verkamp, K. Benke, F. M. F. De Groot, G. S. Girolami and J. Vura-Weis, *J. Phys. Chem. Lett.*, 2016, **7**, 3383–3387.

8 E. S. Ryland, M.-F. Lin, M. A. Verkamp, K. Zhang, K. Benke, M. Carlson and J. Vura-Weis, *J. Am. Chem. Soc.*, 2018, **140**, 4691–4696.

9 E. Stavitski and F. M. F. de Groot, *Micron*, 2010, **41**, 687–694.

10 K. Zhang, G. S. Girolami and J. Vura-Weis, *J. Synchrotron Radiat.*, 2018, **25**, 1600–1608.